2013 IEEE Jordan Conference on Applied Electrical Engineering and Computing Technologies (AEECT)

Histopathological Prostate Tissue Glands Segmentation for Automated Diagnosis

Safa'a N. Al-Haj Saleh
Department of Software engineering
The Hashemite University
Zarqa, Jordan
alhaj.safa@yahoo.com

Omar S. Al-Kadi
King Abdullah II School for IT
The University of Jordan
Amman, Jordan
o.alkadi@ju.edu.jo

Moh'd B. Al-Zoubi
King Abdullah II School for IT
The University of Jordan
Amman, Jordan
mba@ju.edu.jo

Abstract— **In this work, we propose a methodology for segmenting glands automatically in digitized images of histopathological prostate tissue for grade classification. Gleason grading describes the abnormality of cancer cells and their degree of aggressiveness by using numerical scale from grade 1 that represents benign tissues through grade 5 for tissues characterized as advanced stage cancer. The special characteristics of glands in prostate tissue for each grade play a significant role in discriminating Gleason grades. Therefore, lumen objects and tissue glands were segmented as the major regions of interest for tissue grading. Lumen objects were segmented by an empirical thresholding technique. Since we are mainly concerned with the inner regions of the glands consisting of the lumen, cytoplasm and the inner boundary of the cell nuclei, a k-means clustering approach was employed to the a* color channel of the L*a*b* color model for each of the tissue images. This was followed by statistical and morphological features extraction for the segmented lumen objects and glands. Finally, a naive Bayes classifier was used to classify tissue images to the correct grade. The efficiency of the automated segmentation method was evaluated, and classification results achieved accuracy, sensitivity, and specificity of 91.66%, 96.66%, and 95.00%, respectively. These results indicate that our automated methodology could serve as an adjunct to histopathologists and would have a positive impact when integrated with conventional histopathological diagnosis procedures.**

Keywords— Prostate tissue; Gleason grading; gland segmentation; Naive Bayes classifier

I. INTRODUCTION

Prostate cancer (PCa) is a major medical problem that has many economical effects. It is the fifth most common cancer among men in the world. Around 900,000 new cases were diagnosed in 2008 over the world with the percentage of 14% of cancer cases [1]. In Jordan, 133 new cases of PCa were discovered in 2006 with a percentage of 6.5% as compared to all local cancer cases [2]. Early detection of PCa plays a vital role in the treatment of this disease. Some tests are needed to determine whether the patient has PCa or not, and to classify the cancer, if found, into grades. Gleason grading system is the most commonly employed grading system [3]. It relies on the glandular architecture of prostate tissues; describing the degree of loss of the normal glandular tissue architecture (i.e. shape, size and differentiation of the glands). The most prevalent patterns are assigned grades from 1 to 5 where grades 1 and 2 are called benign tissue.

Classifying prostate tissue images into grades based on extracted features from automatically segmented tissue glands is a challenging task that consists of three main stages: Segmentation, feature extraction, and classification. These stages are based on image processing and machine learning techniques.

In the next section, medical background is presented. Related work is discussed in section III. The methodology developed for gland segmentation and tissue classification is discussed in section IV. In section V the results are reported and appropriate discussion is made. Finally, we close this paper with a conclusion in section VI.

II. MEDICAL BACKGROUND

The process of diagnosing PCa consists of several tests. In this work, we are concerned with digitized prostate biopsy tests since it can be easily captured into a high resolution image, which can be then classified using automated approaches. After prostate biopsy is taken, slides of the tissue are prepared and stained using Hematoxylin and Eosin (H&E) staining method [4]. Slides are then scanned using high resolution scanners to be digitized into images that represent the prostate epithelial tissue. The resulting digitized images can be viewed with low resolution (10X) or high resolution (40X) for better analysis. Pathologists can then examine these images to classify tissues into grades. This is based on examining gland units in prostate tissue to check some features such as size, shape, and number of glands in the tissue image.

Prostate gland unit consists of four main components: stroma, lumen, epithelial nuclei, and epithelial cytoplasm. These components appear in different colors in a prostate tissue image stained by the H&E method: stroma is the pink region, lumen is the white region, nuclei are the dark blue dots, and cytoplasm is the purple region.

The special characteristics of glands in each grade of Gleason grading system motivated many researchers to extract features for the glands and for the main components of the

glands for automated diagnosis. In benign tissue (grades 1 and 2), glands are large, appearing as single separated units, having large lumen components and thick gland boundaries with prominent nuclei. There are a lot of variations in lumen shape, from circular to oval or branchy [5]. In grade 3 tissue, glands are smaller and more circular than in a benign pattern. This pattern has also small, circular lumen and thin nuclei boundaries. In grade 4 tissue**,** the glands start to lose their architecture. It is obvious that this grade does not have well-separated gland unit with separate lumen. Nuclei distribute uniformly instead of forming well-defined boundaries as in benign patterns. Glands are fused with each other and they are poorly defined [5]. Multiple glands are mixed together to create a mass of glands containing multiple lumen components. Grade 5 is less common than grade 4. This grade shows variety of patterns with no formation of gland units or lumen appearance [3]. This grade is often undifferentiated; since its features are not significantly distinguishing. For previously mentioned reason, grade 5 is not considered in this research. Figure 1 shows samples of benign, grade 3, and grade 4 tissues.

III. RELATED WORK

Many methodologies were proposed for complete and partial segmentation of glands in prostate tissue image. These methodologies were based on image processing and machine learning techniques such as region growing, level sets, and clustering.

Region growing technique groups pixels of similar features such as intensity or texture into regions. It examines neighboring pixels of initial seed points to check if they should be added to the region or not. Many researchers proposed methodologies for segmenting glands based on region growing technique such as Teverovskiy et al. [6] who developed a medical image analysis system called (MAGIC)

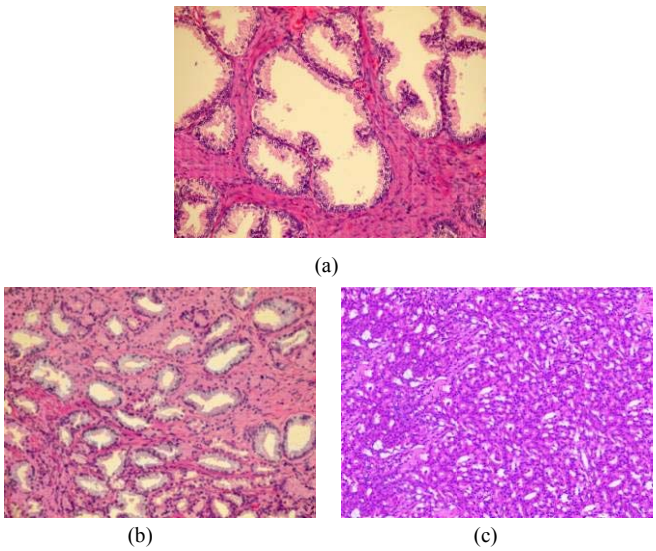

(a) (b) (c)

Fig. 1. Samples of benign and cancerous tissues (a) benign, (b) grade 3, and (c) grade 4.

which was applied specifically to prostate tissue images. Segmentation was done using region growing algorithm that segmented gland objects based on color similarity and shape regularity. Results showed that classification accuracy was 73% on average. Peng et al. [7] also presented a method to segment the complete individual glandular units based on seeded region growing using true lumen regions as the initial seeds. Region growing method was applied iteratively with a 3 × 3 pixel kernel to all seeds. Pixels that belong to stroma were not included in the grown glands. The iterative process ended when all glands stop to grow.

Using region growing techniques for segmenting glands has the advantage of simplicity. It has the disadvantage of consuming computations. In addition, variation of intensities may result in over segmentation. This motivated us to avoid using region growing technique in segmenting glands; due to the heterogeneity of prostate tissue image.

Level set approach was also used to segment the boundaries of glands. This was done by initializing curves that were usually lumen boundaries. These curves evolved to segment the inner or the outer boundary of the gland. Many researchers proposed methodologies for segmenting glands based on level set technique such as Naik et al. [8], Hafiane et al. [9], and Vidal et al [10]. Naik et al. presented an automated glands segmentation method based on low-level information, high-level information and domain-specific information. Low-level information was based on Bayesian classifier to generate likelihood that each pixel belongs to a specific object based on image intensity and textural information. High-level information was based on level set technique to segment gland boundary. Domain-specific information was used to check whether the detected objects were true objects or not based on structural constraints. Tests showed that classification accuracies in distinguishing intermediate grades of PCa were above 90%. Hafiane et al. combined two approaches to develop multiphase vector-based active contours. First approach required multiple levels sets; one for each class in the tissue (lumen, cytoplasm, nuclei, and stroma). Second approach was based on multiple phases of a single level set to detect nuclei centers. Results showed that detection rate was 91% compared to manual detection. Vidal et al. proposed a method that was based on lumen centered expansion by using level set and cell density localization (where cell was used to describe nucleus) by using mean filtering technique. The contour of lumen area was used as the initial zero contour for applying level set for the first time. The curve grew freely involving pixels except nuclei pixels. A second level set was applied to get the complete gland by involving nuclei pixels.

In this work, we chose not to apply level sets to segment glands due to the heterogeneity of prostate tissue image (i.e. the diversity of shape and position of the main parts of a gland), since we intended to avoid defining many initial boundaries to segment glands that would render the technique semi-automated.

In clustering based techniques, gland components were assigned into clusters based on similarity between

components. Many researchers proposed methodologies for segmenting prostate tissue glands based on clustering techniques such as Farjam et al. [11] who proposed a method to segment prostate glands in the image by applying texture based techniques along with clustering techniques. He noticed that lumen and stroma have higher illuminations compared to nuclei. Based on that, values of texture features for lumen and stroma regions was higher than nuclei regions. K-means clustering was applied to segment stroma, lumen, and nuclei. The selected number of clusters was two: one for lumen and stroma and the other for nuclei. Nuclei regions were excluded from stroma and lumen to get glandular regions. Results showed that classification accuracy was around 95%.

Due to simplicity and high speed of clustering techniques, k-means clustering was chosen in this work to segment inner regions of glands. Number of clusters was determined correctly to achieve high segmentation accuracy.

IV. Methodology of Glands Segmentation and Tissue Classification

In this work, we aim to segment lumen objects and tissue glands. We focus on partial gland segmentation by segmenting the inner region of the gland; which consists of lumen, cytoplasm and inner boundary of nuclei. This is done to have good separation of glands since glands in grade 4 tissue tend to fuse to form gland mass. Our purpose is to segment glands separately instead of segmenting combined glands especially when glands are close together or when having gland masses. This improves the accuracy of segmenting the glands. Figure 2 summarizes the general architecture of the proposed methodology for segmentation and classification.

A. Preprocessing Prostate Tissue Images

Filtering H&E prostate tissue image is an essential step for preparing the image for segmentation step. Gaussian filter is applied to smooth the images. It is applied because we focus on region based segmentation not on boundary based segmentation. The general formula of Gaussian function in two dimensions is [12]:

$$G(x,y) = \frac{1}{2\pi\sigma^2} e^{-\frac{x^2+y^2}{2\sigma^2}} \quad (1)$$

where x is the distance from the origin in the horizontal axis, y is the distance from the origin in the vertical axis, and σ is the standard deviation of the Gaussian distribution.

Many filters were tested on prostate tissue images. Gaussian filter showed good smoothing results when applied on dataset

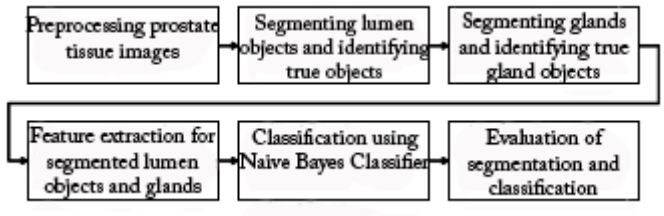

Fig. 2. The general architecture of the proposed methodology

used in this work with $\sigma = 0.71$.

B. Segmenting Lumen Objects and Identifying True Objects

In this work, we focus on segmenting lumen objects as well as segmenting tissue glands. This is done to extract features from lumen objects and glands to have more accurate classification. We start segmenting lumen objects by converting the filtered RGB tissue image into grayscale image. This is done to apply manual thresholding technique for lumen segmentation; since thresholding deals with different intensities of grayscale image [13]. Manual thresholding is based on choosing single parameter known as the intensity threshold. It divides the tissue image in two classes: foreground (lumen objects) and background (other tissue components).

Segmented tissue image *g(x,y)* by applying threshold can be defined as[14]:

$$g(x,y) = \begin{cases} 1 & if \quad f(x,y) > T \\ 0 & if \quad f(x,y) \le T \end{cases} \quad (2)$$

where *f(x,y)* is point of the gray image pixels and *T* is the threshold value.

Trial and error approach is used to empirically choose intensity threshold value that is suitable to segment lumen objects for all types of prostate tissue images. By relying on this approach, we find that the value of 205 is the suitable threshold value. Finally size constraint is applied to keep true lumen objects and eliminate too small detected lumen objects (false lumen objects). The value of the applied size constraint is determined empirically by choosing the suitable value for all tissue types which is 900 pixels.

C. Segmenting glands and identifying true gland objects

Segmenting inner regions of glands starts with converting the filtered RGB tissue image into L*a*b* color model and separating a* channel. Lab color is chosen because it is a perceptually uniform color space. It is designed to approximate the color perception in human visual system [15]. It is used to enhance the separation of different colors of tissue components; i.e. lumen, cytoplasm, nuclei and stroma. We have noticed that lumen and cytoplasm are distinguished from nuclei and stroma in a* image for benign, grade 3, and some grade 4 cases. Based on that, segmentation of inner gland region is performed using extracted a* channel.

After that, k-means clustering is applied on the extracted a* tissue image for initial segmentation of glands. We apply k-means algorithm with three specified parameters: number of clusters *k*, cluster initialization, and distance metric. Number of clusters is two: A cluster that represents lumen and cytoplasm pixels and another cluster that represents nuclei and stroma. Clusters are initialized with tested values that represent the average of luminance values of selected pixels in

each cluster for samples of a* tissue images. Euclidean distance is the distance measure used to assign each pixel in the tissue image to the closest cluster center.

While segmenting the inner region of glands, some holes may occur due to the heterogeneity of prostate tissue; some pixels within the inner region could belong to stroma or nuclei cluster not to lumen or cytoplasm cluster resulting in these holes. To overcome this problem, morphological closing operation is applied on initially segmented glands to fill holes and small gaps. A disk structuring element with small size is used while applying closing operation.

Finally, size constraint is applied to keep true glands. This is important to eliminate too small detected glands (false glands). The value of the applied size constraint is determined empirically by choosing the suitable value for all tissue types which is 2000 pixels. Figure 3 shows the corresponding segmented lumen objects and glands for tissue samples shown in Figure1. Illustrated images for the segmented lumen objects and glands prove the accuracy of the proposed segmentation methodology.

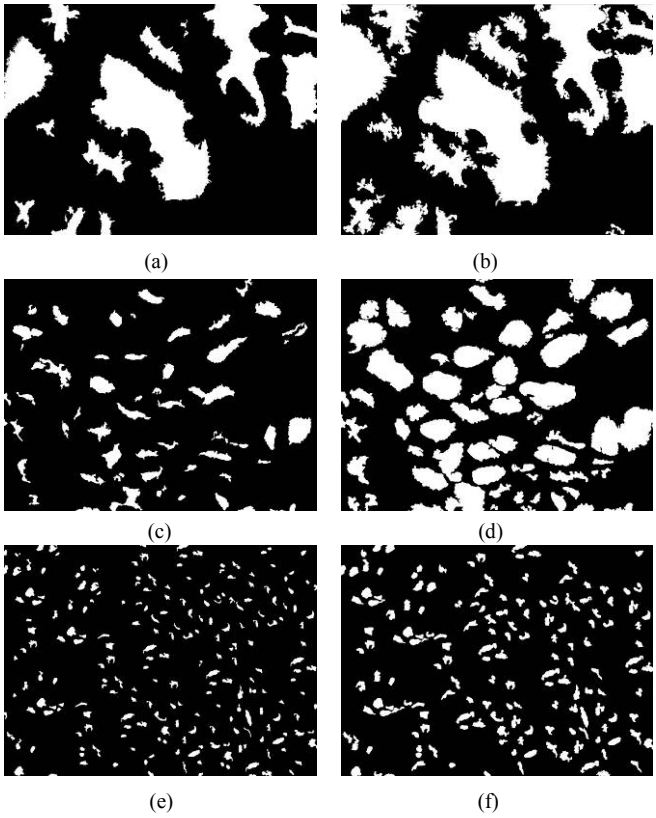

Fig. 3. The corresponding segmented lumen objects (a, c, and e) and the corresponding segmented tissue glands (b, d, and f) for tissue samples (a, b, and c) shown in Figure1, respectively.

D. Feature Extraction for Segmented Lumen Objects and Glands

By the end of segmentation process, final segmented lumen objects and glands are labeled to extract some features necessary to classify tissue image into the suitable grade. As illustrated in Table 1, nine features are extracted for segmented lumen objects and glands. All the extracted features are chosen carefully to have an accurate classification of prostate tissues. Extracted features are classified into statistical features related to area, diameter, and perimeter and morphological features related to eccentricity.

E. Classification Using Naive Bayes Classifier

After extracting features, classification of tissue images is done using naive Bayes classifier, which is known to be a simple probabilistic classifier that assumes features are independent given a specific class. This classifier has the advantage of oversimplifying assumptions; and could give very good accuracy results as compared to other approaches [16]. Evaluation of segmentation and classification is done to prove the accuracy of the proposed methodology as discussed in the results section.

V. RESULTS AND DISCUSSION

All experiments were applied on a dataset that contained digitized H&E prostate tissue images. These images were acquired by preparing prostate biopsy to be ready for digitization through the following steps [17]: fixation, dehydration, clearing, embedding, sectioning, H&E staining, and cover slipping. Number of selected patients was 38 male. They were 22-65 years old. Tissue images were provided from University of Jordan Hospital and Prince Hamza Hospital through ethical approval.

Dataset contained 150 images having the three tissue types: 59 benign tissue images, 41 grade 3 tissue images, and 50 grade 4 tissue images. The grading of these images was confirmed by a pathologist. All tissue images have same size (3136 x 2352) and same magnification (20X). Dataset was divided into training dataset and testing dataset. Training dataset contained 90 tissue images of all tissue types. Testing dataset contained 60 tissue images of all tissue types. This was based on holdout validation, where 2/3 of dataset is chosen for

TABLE I. Features Extracted from Segmented Lumen Objects and Glands

Feature Type	Extracted Features
Lumen Objects Features	Average lumen area, maximum lumen area, and average lumen eccentricity.
Glands features	Average glands area, maximum gland area, average glands diameter, average glands perimeter, average glands eccentricity, and glands density.

training and 1/3 of dataset is chosen for testing. All tests were performed using Matlab 7.8.0 (R2009a) running on a machine of 4 GB RAM and 2.40 GHz core i5.

Many experiments were performed to test the accuracy of the proposed segmentation approach. Images subtraction is one of the simplest ways to view the accuracy of segmentation. It depends on viewing the difference between manually segmented image (reference image) and automatically segmented image. This was done on samples of images that represent all tissue types. Subtracted images for these samples showed high accuracy of segmentation approach. We also calculated correlation r between reference image and automatically segmented image. This was done by computing the correlation coefficient for samples of tissue images[18]:

$$r = \frac{\sum_m \sum_n (A_{mn} - \overline{A})(B_{mn} - \overline{B})}{\sqrt{(\sum_m \sum_n (A_{mn} - \overline{A})^2)(\sum_m \sum_n (B_{mn} - \overline{B})^2)}} \quad (3)$$

where A is the reference image, B is the automatically segmented image, $\bar{A}$ is the mean of A, and $\bar{B}$ is the mean *of* B.

We calculated lumen segmentation accuracy and gland segmentation accuracy for samples of tissue images based on the calculated correlation coefficient. Lumen segmentation accuracy was: 93.45%, 85.21%, and 82.69% for benign, grade 3, and grade 4 tissue samples, respectively. Gland segmentation accuracy was: 84.80%, 84.78%, and 86.41% for benign, grade 3, and grade 4 tissue samples, respectively.

Classifying prostate tissue dataset using naive Bayes classifier resulted in accuracy, sensitivity, and specificity of 91.66%, 96.66%, and 95.00%, respectively. Sensitivity is related to the ability of the classifier to identify positive results. It is the proportion of people who have cancer but classified as positive cases. More specifically, it is the probability of a positive test, given that the patient is ill. Specificity is related to the ability of the classifier to identify negative results. It is the proportion of people who are well but classified as negative cases. More specifically it is the probability of a negative test, given that the patient is well. Some cases that were misclassified are shown in figure 4. This misclassification could be due to some benign cases having morphological characteristics resembling grade 3 cases. Defects in the staining could be another reason for having some misclassified cases.

Our results show that the proposed approach is successful in segmenting H&E prostate tissue images to label lumen objects and glands. Classification accuracy, sensitivity, and specificity show that the extracted features are capable of discriminating different Gleason grades of PCa.

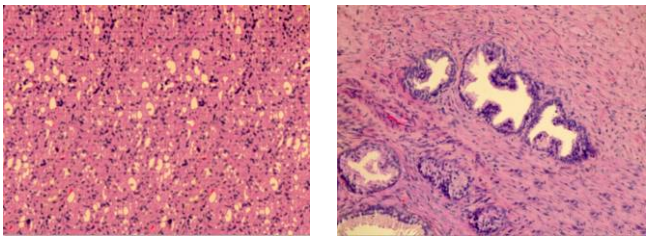

(a) (b)

Fig. 4. Some cases that were misclassified (a) Grade 4 tissue that was misclassified to grade 3. (b) Benign tissue that was misclassified to grade 3.

Our proposed methodology has proven its accuracy and efficiency when comparing sensitivity and specificity values with other methodologies such as Wang et al. [19], Monaco et al. [20], and Xu et al. [21] methodologies. Table 2 compares sensitivity and specificity of the proposed methodology with other methodologies.

VI. CONCLUSION

In this work, we have proposed a fully automated inner gland segmentation, feature extraction, and classification methodology for digitized images of histopathological prostate tissues. The classification of images was based on Gleason grading system to classify them into grades: benign, grade 2, or grade 3. To extract required features for grading the tissues, we focused on segmenting lumen objects and glands. Segmenting lumen objects was performed by an empirical thresholding technique. We were interested in segmenting inner regions of the glands using k-means clustering technique applied to the a* channel of the L*a*b* color model for each tissue image. Nine features were extracted for segmented lumen objects and glands, and then fed to a naive Bayes classifier to classify the tissue images to the appropriate grade.

Main contributions of this work are:

- A new proposed methodology for segmenting glands.
- A fully automated lumen and inner-region glands segmentation, feature extraction and classification.
- Evaluation of segmentation accuracy by images subtraction and correlation coefficient calculation for samples of tissue images.

TABLE II. Sensitivity and Specificity Comparison

Methodology	Sensitivity	Specificity
The proposed methodology	97.56%	96.34%
Wang et al. methodology	87.74%	94.82%
Monaco et al. methodology	82.00%	71.00%
Xu et al. methodology	71.00%	95.00%

For future work, we aim to apply other classification algorithms to the extracted features. Our goal is to test the accuracy of segmentation by comparing the resulting accuracy, specificity, and sensitivity using the naive Bayes algorithm with other classifiers. We also aim to apply the proposed methodology on other datasets from different hospitals.

ACKNOWLEDGMENT

The authors would like to thank Dr. Fatima Obeidat and Dr. Khalid Wissam from the University of Jordan Hospital and Mr. Ali Dumour from Prince Hamza Hospital for their great help in providing, digitizing, and diagnosing the dataset of prostate tissue images.

REFERENCES

[1] A. Jemal et al., "Global cancer statistics" , CA: A Cancer Journal for Clinicians, vol. 61, issue 2, 2011, pp. 69-90.

[2] M. Taraweneh and O. Nimri, "Cancer incidence in Jordan 2006", Jordan Cancer Registry, 2006.

[3] E.A. Tanagho and J.W. McAninch, "Smith's general urology", McGraw-Hill, 17th edition, 2008.

[4] K. Nguyen, A. K. Jain, and R. L. Allen, "Automated gland segmentation and classification for Gleason grading of prostate tissue images", International Conference on Pattern Recognition, IEEE., 2010.

[5] K. Nguyen, B. Sabata , and A. K. Jain, "Prostate cancer grading: gland segmentation and structural features", Pattern Recognition Letters, 2011.

[6] M. Teverovskiy et al.,"Improved prediction of prostate cancer recurrence based on an automated tissue image analysis system", IEEE, 2004.

[7] Y. Peng et al.,"Computer-aided identification of prostatic adenocarcinoma: segmentation of glandular structures", J Pathol Inform, 2011.

[8] S. Naik, S. Doyle, M. Feldman, J. Tomaszewski , and A. Madabhushi, "Gland segmentation and computerized Gleason grading of prostate histology by integrating low-, high-level and domain specific information", MIAAB Workshop, 2007.

[9] A. Hafiane, F. Bunyak , and K. Palaniappan, "Clustering initiated multiphase active contours and robust separation of nuclei groups for tissue segmentation", IEEE, 2008.

[10] J. Vidal et al. , "A fully Automated Approach to Prostate Biopsy Segmentation Based on Level-Set and Mean Filtering", J Pathol Inform, 2011.

[11] R. Farjam , H. Soltanian-Zadeh , K. Jafari-Khouzani , and R. Zoroofi, (2007), "An image analysis approach for automatic malignancy determination of prostate pathological images", Clinica Cytometry Society, 2007, pp. 227–240.

[12] G. Shapiro and C. Stockman, "Computer Vision", Prentice Hall, 2011.

[13] R. Gonzalez and R. Woods, "Digital image processing", 3rd Edition, Prentice Hall, 2007.

[14] S. Al-Amri, N. Kalyankar, and S. Khamitkar, "Image segmentation by using threshold techniques", Journal of computing, vol.2, 2010.

[15] R. Kaur, S. Gupta, and P. Sandhu , "Optimization color quantization in L*a*b* colorspace using particle swarm optimization", Proceedings of International conference on Intelligent Computational Systems, 2011.

[16] R. Caruana and A. Niculescu-Mizil, "An empirical comparison of supervised learning algorithms", Proceedings of the 23rd international conference on Machine learning, CiteSeerX, 2006.

[17] S. He.witt, F. Lewis, Y. Cao, R. Conrad , and M. Cronin , "Tissue handling and specimen preparation in surgical pathology", Arch Pathol Lab Med, vol. 132, 2008.

[18] S. David, "Computation of correlation coefficient and its confidence interval in SAS", SUGI 31, 2009.

[19] Z. Wang et al., "Extraction of prostatic lumina and automated recognition for prostatic calculus image using PCA-SVM", Computational and Mathematical Methods in Medicine,2011.

[20] J. Monaco et al., "Probabilistic pairwise Markov models: application to prostate cancer detection", Proceedings of SPIE, 2009.

[21] J. Xu et al.,"High-throughput prostate cancer gland detection, segmentation, and classification for digitized needle core biopsies", Springer-Verlag Berlin Heidelberg, 2010, pp. 77-88.